



Cite this: *Environ. Sci.: Atmos.*, 2023, 3, 1439

## Real world ultrafine particle emission factors for road-traffic derived from multi-year urban flux measurements using eddy covariance

Agnes Straaten,  Minh-Hien Nguyen and Stephan Weber \*

Vehicular traffic is an important source of ultrafine particles in urban areas. The emission strength may be quantified using particle emission factors (EF) which are an important input to air-quality models such as dispersion or chemical transport models. We quantified particle EFs for a mixed traffic fleet from size-resolved particle number flux measurements in the size range  $10 \text{ nm} < D_p < 200 \text{ nm}$  utilizing the eddy covariance technique at an urban site in Berlin, Germany over the time period from 2017–2020. Particle EFs were calculated using a linear regression approach of particle number fluxes vs. traffic intensity. For the 3 year observation period the average total particle number emission for the mixed fleet ( $\overline{EF}_{mf}$ ) was  $2.80 \times 10^{14} \text{ veh}^{-1} \text{ km}^{-1}$ . The strongest particle emission occurred in the nucleation mode ( $D_p < 30 \text{ nm}$ ), *i.e.* 69% of total mixed fleet particle emission. A multiple regression analysis for light (LDV) and heavy duty vehicles (HDV) indicated higher  $EF_{HDV}$  by a factor of 11.2 for ultrafine particles ( $D_p < 100 \text{ nm}$ ) than  $EF_{LDV}$ , and a factor 9.8 for nucleation mode particles. The eddy covariance particle flux measurements proved a powerful approach to quantify size-resolved particle EFs over multiple years.

Received 2nd May 2023  
Accepted 3rd August 2023

DOI: 10.1039/d3ea00062a

rsc.li/esatmospheres

### Environmental significance

Elevated urban concentrations of ultrafine particles (UFP) are mainly due to significant emission from vehicular road traffic. The emission strength of UFP may be quantified using particle emission factors (EF) which are an important input to air-quality models. Due to the variation of influencing factors such as vehicle type, driving patterns, or specific traffic situations, reported EF span a wide range of values and therefore increase uncertainty of modelled concentration estimates. We derived EF from 3 years of micrometeorological particle number flux observations representing a real-world urban mixed traffic fleet. About 2/3 of traffic particle emission occurred in the nucleation mode  $< 30 \text{ nm}$ . Heavy duty vehicles emitted about 11 times more particles than light duty vehicles. Such longer-term observations certainly help to understand variation in EF and to monitor effects of the modernisation of the traffic fleet.

## 1 Introduction

Cities are characterised by high number concentrations of airborne particles, typically with a share of more than 80–90% of ultrafine particles (UFP, diameter  $D_p < 100 \text{ nm}$ ) in the total number concentration of particles.<sup>1</sup> Vehicular road traffic is reported to be the dominant source of UFP in urban areas, mainly due to significant tailpipe emission of particles in the nucleation size range  $D_p < 30 \text{ nm}$ .<sup>2–4</sup> Although evidence on the impact of UFP on human health from epidemiological studies is inconclusive<sup>5</sup> there are clear indications for human health threats due to elevated UFP exposure.<sup>6</sup> Hence, the European Commission recently issued a revision of the air quality directive, in which regular monitoring of UFP number concentrations at selected sites throughout Europe is proposed in order to

collect data for health-related and epidemiological research on a routine basis.<sup>7</sup>

The emission strength of particles from vehicular road traffic is usually quantified using particle emission factors (EF) for specific vehicle types or mixed fleets such as composed of light and heavy duty vehicles, or cars of different fuel types. A number-based EF specifies the particle number as emitted per vehicle (veh) and unit distance or unit of burned fuel, *e.g.* particles per veh per km or particles per kg of fuel. Particle EFs in different diameter size ranges have been quantified using methods either under controlled laboratory conditions or in real-world situations such as car tunnels, street canyons, along motorways or in urban areas.<sup>8–12</sup> The most common methods to derive EFs are dynamometer measurements, different gaseous traffic tracer methods (*e.g.*  $\text{NO}_x$  tracer method), on-road chasing experiments, inverse modelling approaches or using eddy-covariance flux data.<sup>13–16</sup> The EFs are important input data to air quality models, *e.g.* dispersion models, to implement the source strength of road traffic and subsequently calculate

*Climatology and Environmental Meteorology, Institute of Geoecology, Technische Universität Braunschweig, Langer Kamp 19c, 38106 Braunschweig, Germany.*  
E-mail: s.weber@tu-braunschweig.de



atmospheric transformation and spatial distribution of particle concentrations.

Reported real-world emission factors, however, span a wide range of values, mainly due to the variation of influencing factors in the different research studies such as fuel and vehicle type, driving patterns, vehicle age, topography of the study area, meteorological conditions, or the measured particle size range.<sup>17,18</sup> Many studies also look at relatively short study periods of a few weeks or months and therefore may not capture the range of variation in influencing factors, *e.g.* meteorological conditions.<sup>16</sup> Hence, to better understand the variation of particle EFs, longer observation periods in urban areas are vital. Eddy covariance is a technique to measure the vertical surface-atmosphere exchange of energy or pollutants by a direct approach, *i.e.* without assumptions about the turbulent state of the atmosphere. In combination with traffic data, the measured surface-layer turbulent transport of particles can be utilised to derive emission factors representing the flux source area upwind of the eddy covariance site. Depending on the measurement height and the turbulent state of the atmosphere, the flux source area typically covers a surface area of about  $10^2$  to  $10^4$  m.<sup>19</sup> This provides the opportunity to quantify urban road traffic EFs under real-world conditions from measured particle fluxes, *i.e.* for a mixed vehicle fleet with varying traffic driving patterns such as free flowing traffic or congested conditions. Multi-year measurements enable to study temporal variation, which might point to emission trends in the mixed vehicle fleet or help to assess the effects of traffic mitigation strategies.

In the present study, a 3 year data set of size-resolved particle fluxes from an urban site in Berlin covering the time period 2017–2020 was used to derive traffic emission factors for particles in the size range  $10 \text{ nm} < D_p < 200 \text{ nm}$ . To date, only very few studies are available which report findings from multiple years of eddy covariance particle fluxes and provide size-resolved information on particle EFs.<sup>20</sup> We hypothesise that long-term eddy-covariance observations are a very valuable method to derive particle EFs for a mixed urban fleet covering a large variation of boundary conditions such as driving patterns, turbulent transport and meteorological conditions. We aim to quantify a ‘typical’ mixed-fleet road traffic emission factor which is representative for urban Berlin or other large German cities with similar fleet compositions. Hence, we excluded periods with ‘non-typical’ traffic situations such as weekends or holidays and focussed our analysis on the case of an average weekday situation. Particle EFs are reported for size integrated number concentrations such as ultrafine and total particle number concentrations as well as for concentrations in the nucleation, Aitken and accumulation modes.

## 2 Material and methods

### 2.1 Study site

Size-resolved particle number fluxes were measured at rooftop of the main building of Technische Universität Berlin, Germany in the time period from April 2017–March 2020 (Fig. 1). The site is part of the Urban Climate Observatory Berlin<sup>21</sup> and located at a height of 47 m above ground level (agl). The mean building

height in the vicinity of the site amounts to approximately 18 m above ground level.<sup>22</sup> An impression of the site surroundings is depicted in the Appendix (Fig. 8). To the north of the site, the main road ‘Straße des 17. Juni’ with an average daily traffic (ADT) of 42 700 vehicles per day (average from Monday–Thursday, data source: ref. 23) is located, which is one of the busiest roads in the vicinity of the site.

The study area was defined as a 2 km radius around the site, since this area contains the 80% contour line of the flux source area in every single of the three observation years as determined by flux source area modelling (*cf.*<sup>20</sup>). For the study area, data of 22 automatic traffic counting stations were available from the Senate Department for the Environment, Urban Mobility, Consumer Protection and Climate Action of the Berlin city administration (red dots in Fig. 1). The data set included continuous traffic counts of the respective road cross-section at each site from the period April 2017–March 2020 for the mixed vehicle fleet and separate counts for heavy (HDV) and light duty vehicles including passenger cars (LDV). The absolute maximum daily sums of traffic counts at the 22 sites range between 30 150 vehicles per day and 68 630 vehicles per day over the study period. The average fraction of HDVs in the study area accounted for about 6–7% of total traffic counts. These traffic time series were used to calculate the spatially distributed traffic activity data for estimation of the particle emission factors (*cf.* Section 2.4).

### 2.2 Instrumentation

Particle number flux measurements were conducted with a fast electrical mobility particle sizer (Engine Exhaust Particle Sizer Spectrometer, EEPS 3090, TSI Inc., Minnesota, USA) and a 3D ultrasonic anemometer (USA-1, Metek GmbH, Elmshorn, Germany). Data from both devices were synchronously sampled with a frequency of 10 Hz and logged by a desktop computer. The ultrasonic anemometer and the sample inlet for particle number size distribution (PNSD) measurements were mounted at the top of a 10 m high hydraulic mast which was located at rooftop. This resulted in a measurement height of about 57 m agl. The sample air was transported through a stainless steel tube with an inner diameter of 0.01 m and a flow rate of  $10 \text{ L min}^{-1}$  towards the EEPS and was dried using a Nafion dryer (MD-700, length 0.9 m, Perma Pure LLC). Although the particle size spectrum of the EEPS ranges from 5.6 to 560 nm, the size range for particle number flux measurements was limited to  $10 < D_p < 200 \text{ nm}$ . This size range reduction was necessary due to the gap-filling procedure according to Meyer-Kornblum *et al.*<sup>24</sup> which results in increased uncertainties in the boundary regions of the PNSD (*cf.* Section 2.2). For further details on the gap-filling procedure and the measurement setup, the authors refer to ref. 20 and 24.

### 2.3 Data handling for particle flux calculation

The PNSDs required for particle number flux calculation were first corrected for particle losses in the sampling line (and the Nafion dryer).<sup>25</sup> Particle number concentrations in specific size channels of the PNSD below the associated EEPS minimum



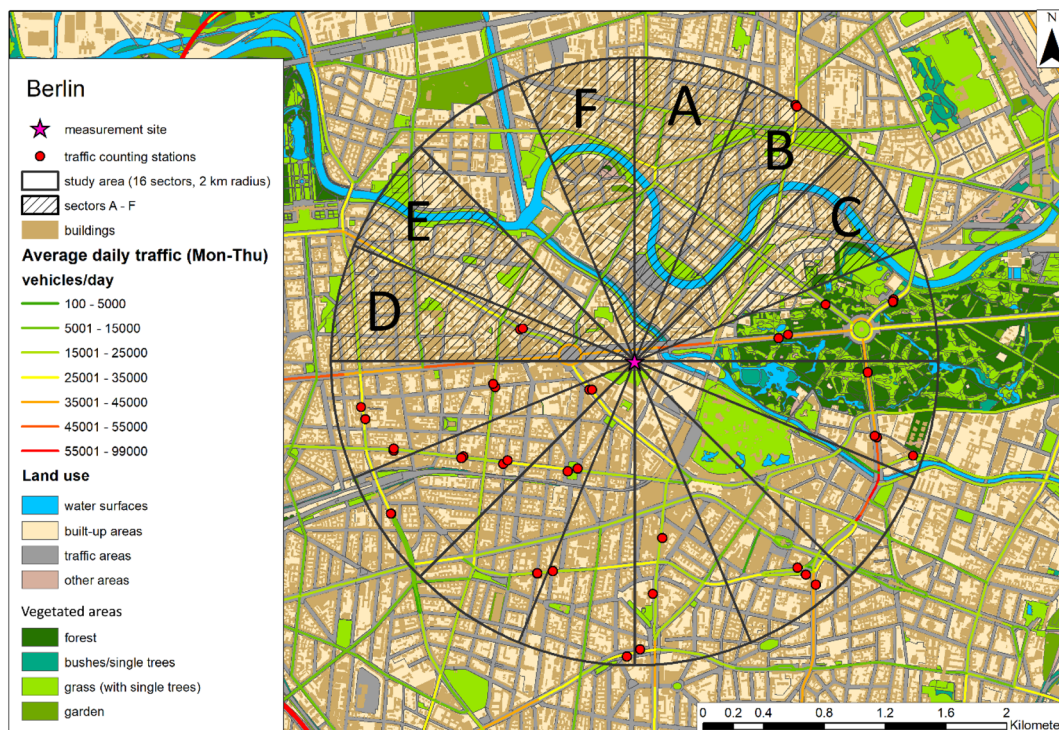


Fig. 1 Study area in Berlin within a radius of 2 km around the flux site. Please note that the average daily traffic (Mon–Thu) is only shown for major roads. Traffic data of the traffic counting stations were provided by the Senate Department for the Environment, Urban Mobility, Consumer Protection and Climate Action of the Berlin city administration (map data sources: ref. 23). Sectors A–F indicate the areas for calculation of particle EFs (cf. Section 2.4).

threshold value were interpolated using a cubic natural spline interpolation method.<sup>24</sup> If too many concentration readings within a PNSD ( $10 \text{ nm} < D_p < 200 \text{ nm}$ ) were below the minimum thresholds ( $>9$  gaps) or were in neighbouring size channels ( $>5$  contiguous gaps), this PNSD was rejected. Overall, 14% of the PNSD data were rejected because of too many gaps in the PNSD. From the remaining 86% of PNSDs, 0.6% were without any gaps and did not require gap-filling, whereas 85.4% of data were gap-filled. According to the analysis of the gap-filling method using the natural spline interpolation<sup>24</sup> the uncertainty in total number concentrations arising from the gap-filling procedure is about 10% for the size range  $10 < D_p < 200 \text{ nm}$ . Our analysis did not point to any bias in the method which tended to a systematic under- or overestimation of particle concentrations by the gap-filling.<sup>20</sup> For these PNSDs size-integrated number concentrations were calculated in order to process particle number fluxes, *i.e.* total particle number concentration (TNC,  $10 \text{ nm} < D_p < 200 \text{ nm}$ ), ultrafine particle number concentration (UFP,  $10 \text{ nm} < D_p < 100 \text{ nm}$ ), nucleation mode particles (NUC,  $10 \text{ nm} < D_p < 30 \text{ nm}$ ), Aitken mode particles (AIT,  $30 \text{ nm} < D_p < 100 \text{ nm}$ ), and accumulation mode particles (ACC,  $100 \text{ nm} < D_p < 200 \text{ nm}$ ).

Several corrections and quality checks were applied for particle number flux calculation, which was performed using EddyPro® v6.2.2 software. The tolerance for missing samples was set to 20%, meaning that there had to be at least 80% data availability in each half-hour period. Furthermore, particle and wind data were checked for plausibility range and spikes were

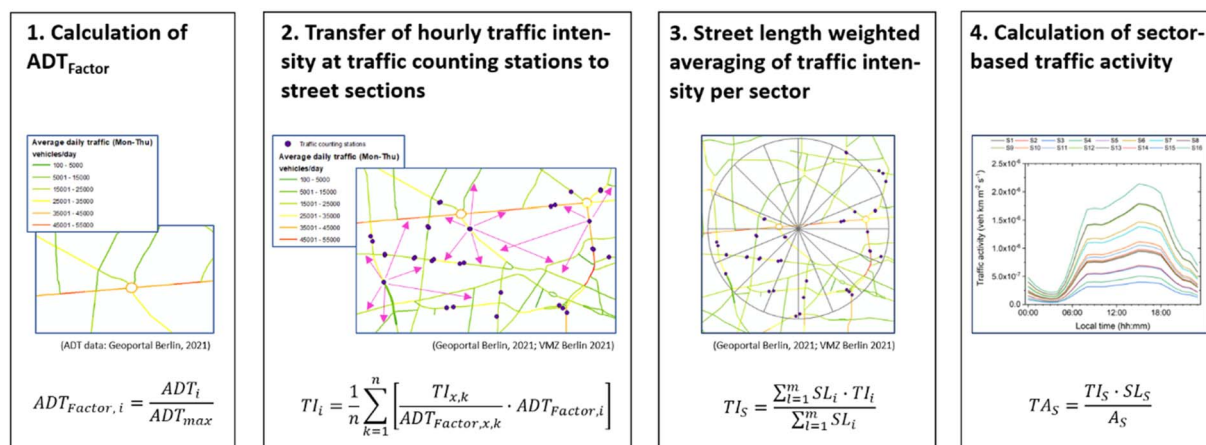
removed.<sup>26</sup> Spectral corrections regarding high-pass and low-pass filter effects were applied using the methods of Moncrieff *et al.*<sup>27,28</sup>. In addition, double coordinate rotation for tilt correction, linear detrending and a time lag correction by covariance maximisation within a specific time lag window ( $9 \text{ s} \pm 4.5 \text{ s}$ ) were used. Underestimation of particle number flux due to EEPs response time was calculated and corrected,<sup>29</sup> while data quality was characterised according to Foken *et al.*<sup>30</sup>. In that respect, particle fluxes with quality flags  $>6$  were discarded. The resulting particle number fluxes are subject to the following sign convention: emission fluxes have a positive sign and are directed to the atmosphere, whereas deposition fluxes are negative and directed to the surface. For further details on data handling, quality control, or data assurance the reader is referred to Straaten *et al.*<sup>20</sup>.

#### 2.4 Preparation of the traffic data set

For the determination of particle emission factors using eddy covariance fluxes, a specific data set with traffic information in the unit  $\text{veh km m}^{-2} \text{ s}^{-1}$  (traffic activity, TA) is needed.<sup>15</sup> To gather this information, the spatial distribution of ADT (data source: ref. 23) in each of the 16 sectors within the 2 km radius (Fig. 1), was combined with hourly traffic data from 22 traffic counting stations located in the study area (Fig. 2).

In the first step, a quantity  $\text{ADT}_{\text{Factor}}$  was obtained for each street section  $i$  of the ADT data set in the 2 km radius using eqn (1)





**Variables:**  $ADT$  = average daily traffic (veh day<sup>-1</sup>),  $ADT_{Factor}$  = relative measure of traffic intensity (-),  $TI$  = traffic intensity (veh h<sup>-1</sup>),  $SL$  = street length (m),  $T$  = traffic activity (veh km m<sup>-2</sup> s<sup>-1</sup>),  $A$  = sector surface area (m<sup>2</sup>),  $n$  = number of traffic counting stations,  $m$  = number of street sections in sector,  $max$  = maximum value in the study area; **Indices:**  $i$  = street section,  $x$  = traffic counting station,  $S$  = sector

Fig. 2 Workflow of the required procedures to calculate a traffic data set for quantification of particle emission factors.

$$ADT_{factor,i} = \frac{ADT_i}{ADT_{max}} \quad (1)$$

with  $ADT_i$  the average daily traffic at a street section  $i$ , and  $ADT_{max}$  the average daily traffic at the busiest road in the 2 km radius. By means of  $ADT_{factor}$ , the temporal variation of traffic data at the counting sites could be spatially transferred to the other street sections of the ADT data set in the next step. Since each traffic counting station  $x$  with index  $k$  can be assigned to a specific  $ADT_{factor}$  ( $ADT_{factor,x,k}$ ), the time-resolved traffic intensity ( $TI$ , in veh per h) for the other street sections were determined by scaling the intensity at the traffic counting sites ( $TI_{x,k}$ ) by the proportion of  $ADT_{factor,i}$  to  $ADT_{factor,x,k}$  (eqn (2)). Averaging over all 22 traffic counting stations ( $n = 22$ ) an hourly-resolved data set of  $TI$  for each street section  $i$  in the study area is provided (cf. Fig. 2).

$$TI_i = \frac{1}{n} \sum_{k=1}^n \left[ \frac{TI_{x,k}}{ADT_{factor,x,k}} \times ADT_{factor,i} \right] \quad (2)$$

For the analysis of particle emission factors on a sector basis,  $TI$  had to be determined at the sector level. Hence, the  $TI_i$  of  $m$  street sections within a sector  $S$  were arithmetically averaged, and weighted by its street length ( $SL_i$ ).

$$TI_S = \frac{\sum_{i=1}^m (SL_i \times TI_i)}{\sum_{i=1}^m SL_i} \quad (3)$$

In the last step, the sector-based traffic activity ( $TA_S$ ) was calculated using the total street length of the sector ( $SL_S$ ) and the sector area ( $A_S$ ).

$$TA_S = \frac{TI_S \times SL_S}{A_S} \quad (4)$$

The resulting data set included hourly traffic data of  $TA$  for the three measurement years for each of the 16 sectors of the study area.

## 2.5 Quantification of road-traffic emission factors

To quantify road traffic related particle emission factors from eddy covariance observations, particle number emission fluxes (*i.e.* positive fluxes, cf. Section 2.2) were subject to linear regression *versus* sector-wise traffic activity  $TA$  for wind sectors strongly influenced by traffic. The linear fit to the data according to eqn (5)<sup>15</sup>

$$F = EF_{mf} \times TA + F_0 \quad (5)$$

identifies the real-world particle emission factor for the mixed vehicle fleet in the study area as the slope ( $EF_{mf}$  in veh<sup>-1</sup> km<sup>-1</sup>) of the linear regression equation.  $F_0$  represents the particle emission flux from other particle sources in the flux source areas excluding road traffic. In case that traffic activity is available for both, LDV and HDV, multiple linear regression can be used to derive particle emission factors for both vehicles types ( $EF_{LDV}$  and  $EF_{HDV}$ ).<sup>15</sup>

$$F = EF_{LDV} \times TA_{LDV} + EF_{HDV} \times TA_{HDV} + F_0 \quad (6)$$

In order to derive robust particle emission factors for urban road traffic, wind sectors must be characterised by significant traffic activity. Here, we selected wind directions sectors which were characterised by high average particle emission fluxes during the three study years (cf. Fig. 9a) and have >20% of traffic land use in the sector flux source area.<sup>20</sup> The sectors meeting this requirements are located to the west and north of the study site (cf. Fig. 1, 270°–67.5°). However, the NW sector located between sectors E and F (315°–337.5°) was excluded due to the occurrence of distinct deposition fluxes (Fig. 9b). We argue that particle deposition and emission fluxes may



appear simultaneously in the urban boundary layer. Thus, a strong emission flux may be reduced by simultaneously occurring particle deposition. Since deposition and emission fluxes in this sector were in the same order of magnitude (cf. Fig. 9), we excluded this sector from further analysis. As a result, six of the 16 sectors (sectors A–F; Fig. 1) were selected for the determination of particle emission factors. However, the remaining sectors were used to evaluate the robustness of  $EF_{mf}$  (cf. Section 3.2). Time periods with lower traffic intensity such as weekends and vacation periods were discarded in order to calculate road traffic emission factors for typical weekday traffic conditions.

Particle emission factors were quantified sector-wise, *i.e.* for each wind direction sector A–F specifically, to study the variation of  $EF_{mf}$  due to different traffic activity per sector. Subsequently, emission factors were also calculated as an average emission factor for the six sectors A–F ( $\overline{EF}_{mf}$ ) to characterise the typical road traffic emission for the study area. The tailpipe and non-tailpipe particle emission from vehicles will be subject to different physical and chemical aerosol transformation processes during turbulent atmospheric transport such as coagulation, condensation and others (*e.g.*<sup>31</sup>). As this study determines emission factors using particle fluxes observed at a receptor site (*i.e.* the eddy covariance site at 57 m agl) we define the resulting emission factor as an effective real-world particle emission factor for road traffic which is not corrected for atmospheric transformation processes.

## 3 Results

### 3.1 Sectoral analysis

Traffic-related particle emission factors in the selected wind sectors A–F were in the range  $1.54 \times 10^{14}$  to  $3.47 \times 10^{14}$   $\text{veh}^{-1} \text{km}^{-1}$  (Fig. 3 and Table 1). The lowest emission factor occurred

**Table 1** Results from the regression of particle fluxes ( $F_{TNC}$ ) vs. sector-wise traffic activity (TA). Sector-wise results are depicted for the road traffic particle emission factor ( $EF_{mf}$ ), the particle emission from other sources ( $F_0$ ) and the coefficient of determination ( $R^2$ ). The average particle emission factor  $\overline{EF}_{mf}$  of all six sectors is also specified. The analysis of variance test (ANOVA) indicated that the regression slopes in all sectors were significantly different from zero (at the  $p = 0.05$  level) and population means of particle fluxes and traffic activity were significantly different (Mann–Whitney test,  $p = 0.05$ )

Sector		$EF_{mf}$ ( $\text{veh}^{-1} \text{km}^{-1}$ )	$F_0$ ( $\text{m}^{-2} \text{s}^{-1}$ )	$R^2$
A	All data	$2.35 \times 10^{14}$	$3.85 \times 10^7$	0.25
	Bin average	$2.36 \times 10^{14}$	$3.61 \times 10^7$	0.95
B	All data	$2.78 \times 10^{14}$	$1.90 \times 10^7$	0.32
	Bin average	$2.81 \times 10^{14}$	$1.92 \times 10^7$	0.96
C	All data	$3.46 \times 10^{14}$	$1.35 \times 10^7$	0.32
	Bin average	$3.09 \times 10^{14}$	$2.63 \times 10^7$	0.98
D	All data	$1.54 \times 10^{14}$	$0.75 \times 10^7$	0.29
	Bin average	$1.45 \times 10^{14}$	$1.56 \times 10^7$	0.99
E	All data	$3.36 \times 10^{14}$	$4.02 \times 10^7$	0.22
	Bin average	$3.28 \times 10^{14}$	$4.20 \times 10^7$	0.99
F	All data	$3.47 \times 10^{14}$	$11.0 \times 10^7$	0.08
	Bin average	$3.80 \times 10^{14}$	$10.20 \times 10^7$	0.89
Average (A–F)	All data	$2.83 \times 10^{14}$	$3.81 \times 10^7$	0.25
	Bin average	$2.80 \times 10^{14}$	$4.02 \times 10^7$	0.96

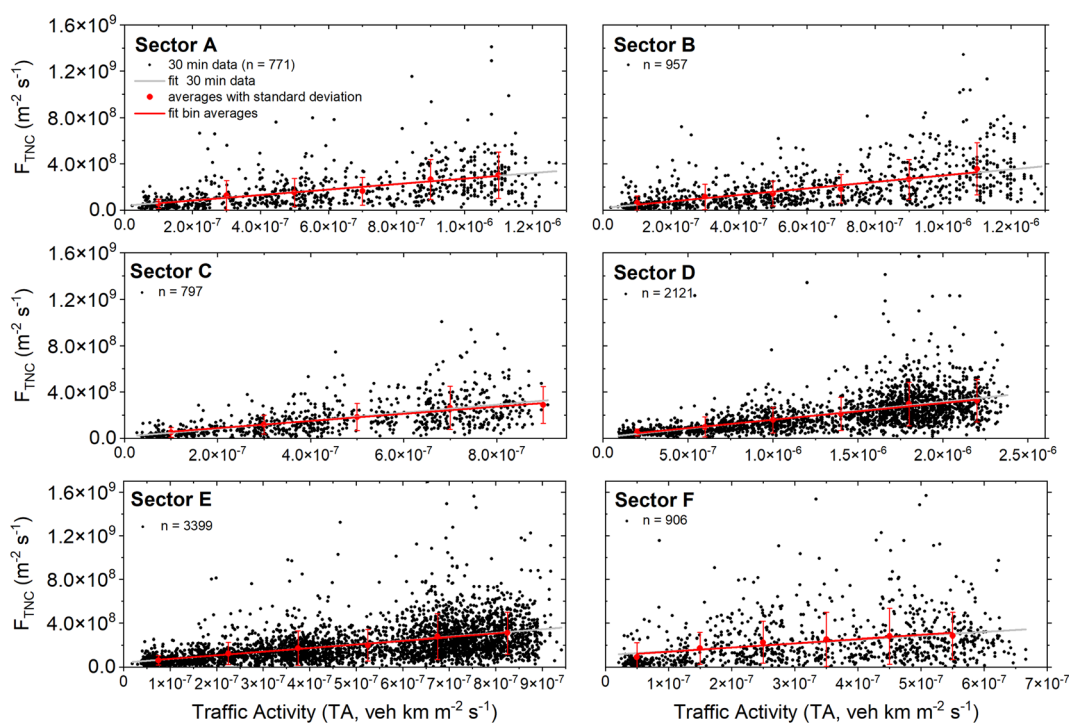


**Fig. 3** TNC fluxes ( $F_{TNC}$ ) as function of traffic activity (TA) for wind direction sectors A–F. Regressions fits (eqn (5)) for the 30 min flux data is indicated by the grey line, whereas the fit to the binned average (red dot with standard deviation as error bars) is indicated by the red line.



in sector D, whereas the highest emission factors were evident in sectors C and F. The  $EF_{mf}$  for binned particle fluxes were in a range of  $1.45 \times 10^{14}$  to  $3.80 \times 10^{14}$   $\text{veh}^{-1} \text{km}^{-1}$  and thus very similar to the emission factors as derived from the regression of half-hourly fluxes *vs.* traffic intensity (Fig. 3 and Table 1). The 30 min data, however, showed distinct variation as indicated by  $R^2 < 0.32$ . The variation during the study period is probably due to different conditions such as weather and turbulent exchange

conditions, driving speeds and driving modes (congested *vs.* flowing traffic).

With exception of sector F, the binned values of  $F_0$  vary between  $0.75 \times 10^7$  to  $4.02 \times 10^7$   $\text{m}^{-2} \text{s}^{-1}$ , which corresponds to 6.3–33.8% of the 3 year average total particle number flux at this site, *i.e.*  $F_{TNC} = 1.19 \times 10^8$   $\text{m}^{-2} \text{s}^{-1}$  (*cf.*<sup>20</sup>). The averaged TNC emission factor for sectors A–F resulted in  $\overline{EF}_{mf} = 2.83 \times 10^{14}$   $\text{veh}^{-1} \text{km}^{-1}$  ( $\pm$  standard deviation of  $0.71 \times 10^{14}$   $\text{veh}^{-1} \text{km}^{-1}$ ) for the 3 year period,

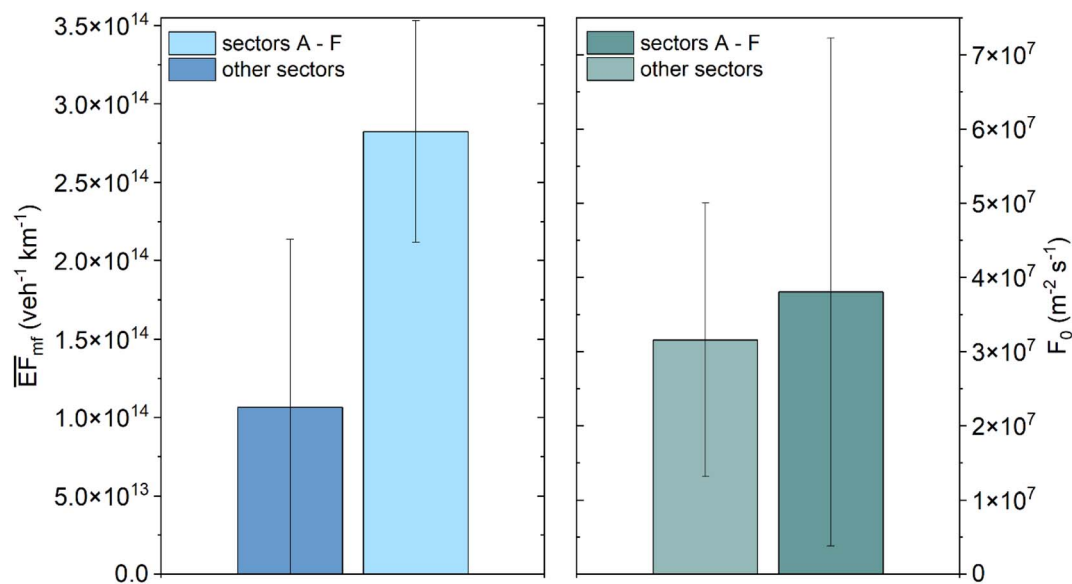


Fig. 4 (a) Average particle emission factors ( $\overline{EF}_{mf}$ ) and (b) average  $F_0$  (standard deviations are shown by error bars) for TNC in sectors A–F and the other sectors. Please note the different y-axis scaling.

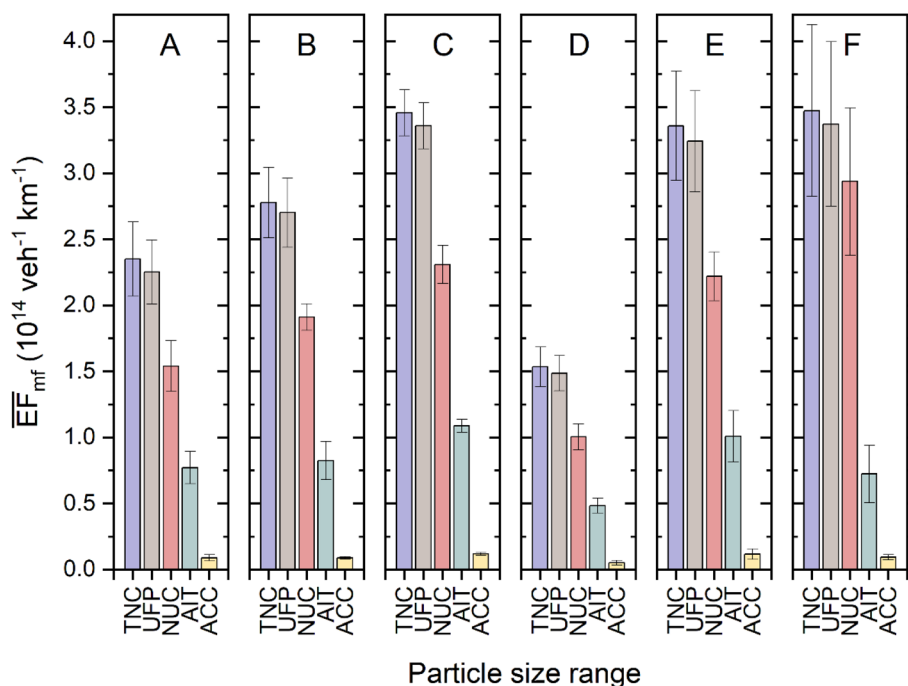


Fig. 5 Size-resolved average particle emission factors for road traffic in sectors A–F calculated from annual estimates. The standard deviation is depicted by error bars.



whereas the average  $F_0$  was  $3.81 (\pm 3.4) \times 10^7 \text{ m}^{-2} \text{ s}^{-1}$  (*i.e.* 32% of 3 year average TNC flux). Since traffic was found to be the main source of ultrafine particles at this site,<sup>20</sup> a (minor) relative share of 6.3–33.8% of particles from other sources than traffic in the different sectors seems plausible. However, the  $F_0$  value of  $11.0 \times 10^7 \text{ m}^{-2} \text{ s}^{-1}$  in sector F is distinctly larger than in the other sectors and nearly in the same order as the 3 year average particle number flux. The reason for the deviation from the other sectors is not yet clear, but might be related to a larger (unknown) particle emission source.

### 3.2 Evaluation of derived $EF_{mf}$

In order to evaluate the robustness of the derived emission factors  $EF_{mf}$ , we applied the method of linear regression (*cf.* Section 2.5) to each of the 16 sectors despite the amount of traffic activity (Fig. 4). While  $\overline{EF}_{mf}$  was higher by a factor of 2.7 in sectors A–F in comparison to the other sectors, the average  $F_0$  values were similar in sectors A–F and the other sectors (factor 1.2). This indicates similar sources of non-traffic particle emission in the 16 wind direction sectors, but higher and more immediate traffic influence in sectors A–F. Thus, the choice of sectors A–F for calculating traffic-related particle emission factors seems reasonable.

### 3.3 Size-resolved analysis and inter-annual variation

The observation of size-resolved particle fluxes at our study site allows for the determination of emission factors for particles in different size ranges, *e.g.* the three modes NUC, AIT, and ACC. Most particles emitted by road traffic in the different sectors were in the nucleation mode, followed by particles in the Aitken mode

(Fig. 5). The averaged emission factors  $\overline{EF}_{mf}$  for sectors A–F were  $1.99 (\pm 0.61) \times 10^{14} \text{ veh}^{-1} \text{ km}^{-1}$  for NUC,  $0.81 (\pm 0.20) \times 10^{14} \text{ veh}^{-1} \text{ km}^{-1}$  for AIT particles, and  $0.09 (\pm 0.02) \times 10^{14} \text{ veh}^{-1} \text{ km}^{-1}$  for ACC mode particles. Thus, the amount of emitted UFP (as the sum of NUC and AIT modes) makes a fraction of 97% of total particles in the size range  $10 \text{ nm} < D_p < 200 \text{ nm}$ . The fraction of particle emission in NUC mode is 69% of TNC. The differences between the sectors A–F with highest emission factors in sector C and F and lowest in D (*cf.* Fig. 3) are also evident for UFP and particle mode emissions (Fig. 5).

The emission factors were characterised by inter-annual variation between the three observation years, *e.g.* the TNC emission factor decreased by about 17% from the first to the second year and increased by about 9% from the second to the third year (Fig. 6).

The coefficient of variation, which is defined as the quotient of the standard deviation and the arithmetic average across sectors A–F, is 26% for TNC. Thus, inter-annual differences of  $\overline{EF}_{mf}$  are lower than the coefficient of variation across wind direction sectors indicating that robust temporal trends cannot be derived from the present data. The inter-annual variation of UFP, NUC, AIT, and ACC particle emission factors were in a similar range as the TNC variation with 26% for UFP, 26% for NUC, 29% for AIT, and 34% for ACC.

### 3.4 Particle emission factors for light-duty and heavy-duty vehicles

To analyse vehicle type-specific particle emission factors, *i.e.* emission factors for LDVs and HDVs, sector-wise multiple linear regression was performed using specific traffic data for LDVs and HDVs. It is evident that HDVs emit significantly more

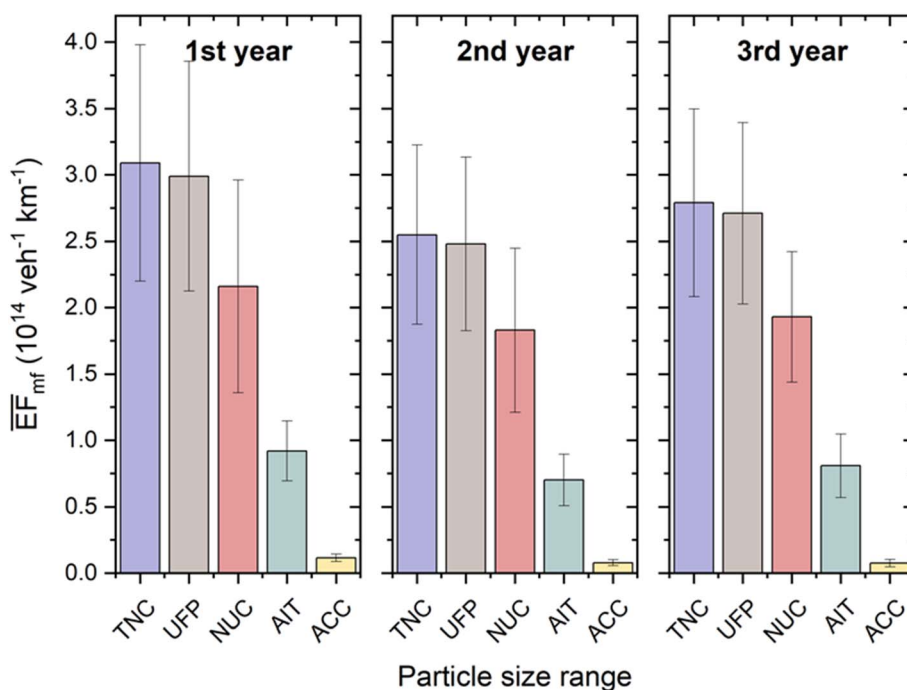


Fig. 6 Size-resolved average particle emission factors ( $\overline{EF}_{mf}$ , with standard deviation) for road traffic in sectors A–F for the three individual measurement years from April 2017 until March 2018 (1st year), April 2018 until March 2019 (2nd year), and April 2019 until March 2020 (3rd year).



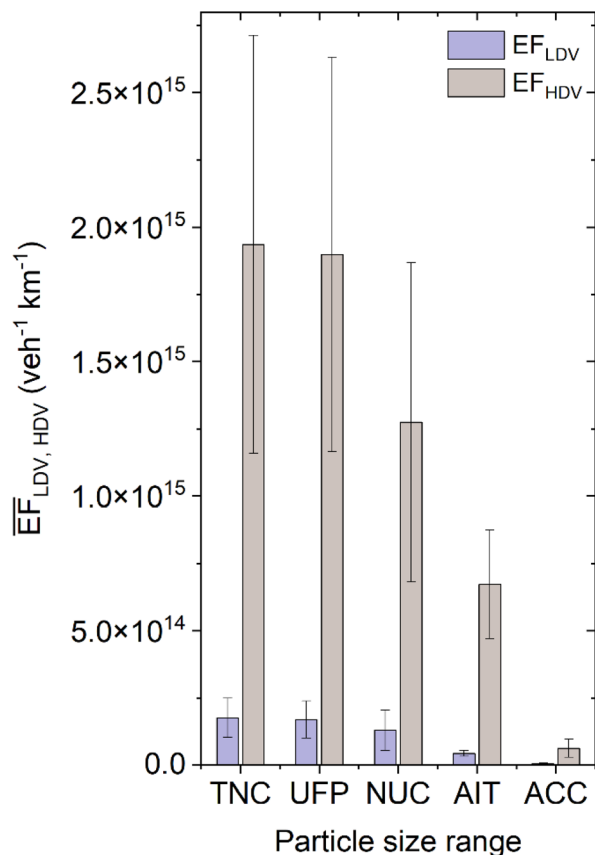


Fig. 7 Size-resolved average particle emission factors (with standard deviation) for light-duty vehicles ( $EF_{LDV}$ ) and heavy-duty vehicles ( $EF_{HDV}$ ) for road traffic in sectors A–F.

particles than LDVs with the ratios of the emission factors for HDV and LDVs varying between  $9.5 < EF_{HDV}/EF_{LDV} < 15.3$  (Fig. 7 and Table 2). The proportion of particle emission in NUC and AIT distinctly differs for LDVs and HDVs. The LDV fleet in Berlin emitted about three quarters of total particles in the NUC mode (*i.e.* 72% of total particles), followed by 25% in the AIT mode. The HDV fleet also dominantly emitted in the NUC mode, however, with 63% emission in the NUC mode the relative share was lower in comparison to the LDV fleet. The HDV fleet emitted 33% of total particles in the AIT mode.

Although the multiple linear regression models to determine  $EF_{LDV}$  and  $EF_{HDV}$  for the sectors A–F were statistically significant at the  $p = 0.05$  level it has to be noted that the predictor variables LDV and HDV were correlated with  $r \approx 0.8$ . Predictor variables with correlation coefficients of  $r > 0.7$  point to collinearity which confines the understanding of the exact relationship between the predictors and response variables but does not impact model predictions (*e.g.*<sup>32</sup>). However, there should be some caution applied when transferring the present MLR estimates to other study sites, especially with different compositions of the traffic fleet such as different fractions of HDV.

## 4. Discussion

### 4.1 Comparison to literature estimates

In the past two decades, particle emission factors for road vehicles have been derived using different methods, *e.g.* on-road measurements, dynamometer measurements,  $NO_x$  tracer method, and turbulent flux measurements applying the eddy covariance technique (*cf.* Table 3 for an overview). Generally,  $EF_{mf}$  is influenced by multiple factors, such as the observed particle size range, fuel and vehicle type, driving patterns, topography, driving behaviour or vehicle age (*e.g.*<sup>18</sup>). Consequently, the determined emission factors span a wide range, with median or average values for mixed vehicle fleets varying from  $0.2$ – $14.6 \times 10^{14} \text{ veh}^{-1} \text{ km}^{-1}$  (Table 3). The present  $EF_{mf}$  for TNC characterising the mixed vehicle fleet in the flux source area around our study site in Berlin varies from  $1.5$ – $3.5 \times 10^{14} \text{ veh}^{-1} \text{ km}^{-1}$  for the different wind direction sectors A–F. This is clearly within the range of  $EF_{mf}$  as reported by others (Table 3).

Due to the considerable emission of UFPs from road traffic,<sup>9,20,33,34</sup> the lower cut-off of particle sizing or counting instruments may explain higher emission factors in case of a lower cut-off size, *e.g.*  $EF_{mf}$  of  $0.9$ – $2.7 \times 10^{14} \text{ veh}^{-1} \text{ km}^{-1}$  with cut-off  $D_p = 8 \text{ nm}$  *vs.*  $EF_{mf}$  of  $1.9$ – $9.9 \times 10^{14} \text{ veh}^{-1} \text{ km}^{-1}$  with cut-off  $D_p = 3 \text{ nm}$  (35; Table 3). Studies having a similar lower diameter cut-off (*e.g.* 9–11 nm) and a similar proportion of HDV in the mixed vehicle fleet compared to our site in Berlin, reported emission factors between  $1.4 \times 10^{14} \text{ veh}^{-1} \text{ km}^{-1}$  and  $2.9 \times 10^{14} \text{ veh}^{-1} \text{ km}^{-1}$ .<sup>9,15,34,36–38</sup> The sector-averaged TNC emission factor of  $\overline{EF}_{mf} = 2.83 (\pm 0.70) \times 10^{14} \text{ veh}^{-1} \text{ km}^{-1}$  as derived from the present data is exactly within this range. However, in contrast to

Table 2 Average size-resolved particle emission factors for the mixed fleet ( $\overline{EF}_{mf}$ ) from linear regression, and light-duty ( $\overline{EF}_{LDV}$ ) and heavy-duty vehicles ( $\overline{EF}_{HDV}$ ) from multiple linear regression.  $F_0$  is representing the particle emission flux from other sources (excluding vehicular traffic). The leftmost  $F_0$  specifies the intercept from the linear regression, whereas the other  $F_0$  gives the intercept from the multiple linear regression.  $\overline{EF}_{HDV}/\overline{EF}_{LDV}$  quantifies the ratio of both emission factors. All values are derived from regression analysis for sectors A–F. Please note the different units

Size	Linear regression			Multiple linear regression				
	$\overline{EF}_{mf}$ ( $10^{14} \text{ veh}^{-1} \text{ km}^{-1}$ )	$F_0$ ( $10^7 \text{ m}^{-2} \text{ s}^{-1}$ )	$R^2$	$\overline{EF}_{LDV}$ ( $10^{14} \text{ veh}^{-1} \text{ km}^{-1}$ )	$\overline{EF}_{HDV}$ ( $10^{14} \text{ veh}^{-1} \text{ km}^{-1}$ )	$\overline{EF}_{HDV}/\overline{EF}_{LDV}$	$F_0$ ( $10^7 \text{ m}^{-2} \text{ s}^{-1}$ )	$R^2$
TNC	2.83 ( $\pm 0.77$ )	3.81 ( $\pm 3.42$ )	0.25	1.77 ( $\pm 0.73$ )	19.35 ( $\pm 7.76$ )	10.9	3.66 ( $\pm 3.50$ )	0.27
UFP	2.74 ( $\pm 0.75$ )	3.71 ( $\pm 3.45$ )	0.25	1.69 ( $\pm 0.69$ )	18.98 ( $\pm 7.32$ )	11.2	3.57 ( $\pm 3.53$ )	0.27
NUC	1.99 ( $\pm 0.67$ )	2.40 ( $\pm 2.61$ )	0.22	1.30 ( $\pm 0.75$ )	12.74 ( $\pm 5.93$ )	9.8	2.31 ( $\pm 2.66$ )	0.25
AIT	0.82 ( $\pm 0.22$ )	1.79 ( $\pm 0.81$ )	0.19	0.44 ( $\pm 0.11$ )	6.72 ( $\pm 2.01$ )	15.3	1.75 ( $\pm 0.84$ )	0.21
ACC	0.09 ( $\pm 0.02$ )	0.35 ( $\pm 0.06$ )	0.15	0.06 ( $\pm 0.02$ )	0.62 ( $\pm 0.33$ )	10.3	0.34 ( $\pm 0.06$ )	0.17



Table 3 Overview of particle emission factors for road traffic from various studies with different methodologies

Location/study	Size range (nm)	Emission factors ( $10^{14}$ veh $^{-1}$ km $^{-1}$ )			Fraction of HDV (%)	Method
		EF <sub>mf</sub>	EF <sub>LDV</sub>	EF <sub>HDV</sub>		
Copenhagen (Denmark) <sup>36</sup>	10–700	$2.8 \pm 0.5^a$	—	—	6–8	Roadside measurements with inverse modelling (street canyon)
Minnesota (Minneapolis, USA) <sup>35</sup>	8–300	0.9–2.7	—	—	9 <sup>b</sup>	On-road measurements (motorway)
Brisbane (Australia) <sup>13</sup>	15–700	$1.11 \pm 0.90^c$ (Tora St) <sup>l</sup>	—	—	6	On-road measurements with box model
	15–700	$0.57 \pm 0.28^c$ (Ipswich Rd) <sup>m</sup>	—	—	15	
Minnesota (Minneapolis, USA) <sup>39</sup>	>3	—	$6.2 \pm 1.4^d$	$42.0 \pm 6.0^d$	—	On-road measurements (motorway)
Stockholm (Sweden) <sup>15</sup>	8–300	—	$0.34 \pm 0.05^d$	$6.6 \pm 1.0^d$	—	Eddy covariance (lin. regression with traffic activity)
	>11	$1.4 \pm 0.2^e$	$0.3 \pm 0.3^e$	$19.8 \pm 4.0^e$	6	
Berlin (Germany) <sup>9</sup>	10–500	$2.1 \pm 0.2^a$	$0.24 \pm 0.15^a$	$29.6 \pm 3.5^a$	6	Roadside measurements with inverse modelling (motorway)
	10–50	$1.3 \pm 0.2^a$	—	—	—	Eddy covariance (footprint estimation, traffic rate)
Helsinki (Finland) <sup>42</sup>	6–5000	$3.0 \pm 1.1^f$	—	—	—	NO <sub>x</sub> tracer method (motorway and urban street)
Copenhagen (Denmark) <sup>37</sup>	10–700	$2.15 \pm 0.05^d$ (motorway)	$0.81 \pm 0.07^d$ (motorway)	$17.5 \pm 0.68^d$ (motorway)	8	
		$1.87 \pm 0.03^d$ (urban street)	$1.01 \pm 0.06^d$ (urban street)	$22.06 \pm 1.28^d$ (urban street)	—	
Lecce (Italy) <sup>38</sup>	9–1000	$2.9 (2.2–5.0)^g$	—	—	—	Eddy covariance (footprint estimation, traffic rate)
Boston (Massachusetts, USA) <sup>43</sup>	4–3000	Southbound tunnel: $5.1 \pm 2.3^h$	—	—	2–5 <sup>b</sup>	On-road measurements (motorway tunnel)
		Northbound tunnel: $1.4 \pm 0.42^h$	—	—	1–3 <sup>b</sup>	
Meckenheim (Germany) <sup>40</sup>	14–750	3.7	2.1	11.8	18	NO <sub>x</sub> tracer method (motorway)
	14–50	3.1	1.6	10.9	—	
	14–100	3.5	1.9	11.4	—	
	50–200	0.6	0.5	0.7	—	
Londrina (Brazil) <sup>18</sup>	>10	$14.6^i$	$9.25 \pm 1.13^d$	$37.28 \pm 5.79^d$	13	Roadside measurements with inverse modelling (street canyon)
Lecce (Italy) <sup>34</sup>	9–3000	$2.2 \pm 0.62^d$	—	—	—	Eddy covariance (footprint estimation, traffic rate)
Mumbai (India) <sup>44</sup>	>10	$0.21 \pm 0.05^j$	—	—	2	On-road measurements (motorway tunnel)
Berlin (Germany)/this study	10–200	$2.83 \pm 0.70^j$ (1.54) <sup>k</sup>	$1.77 \pm 0.73^j$ (1.01) <sup>k</sup>	$19.36 \pm 7.77^j$ (10.37) <sup>k</sup>	6	Eddy covariance (lin. regression with traffic activity)
	10–100	$2.74 \pm 0.69^j$ (1.49) <sup>k</sup>	$1.69 \pm 0.69^j$ (0.97) <sup>k</sup>	$19.00 \pm 7.33^j$ (10.30) <sup>k</sup>	—	
	10–30	$1.99 \pm 0.61^j$ (1.00) <sup>k</sup>	$1.30 \pm 0.75^j$ (0.61) <sup>k</sup>	$12.74 \pm 5.93^j$ (7.70) <sup>k</sup>	—	
	30–100	$0.81 \pm 0.20^j$ (0.48) <sup>k</sup>	$0.44 \pm 0.11^j$ (0.36) <sup>k</sup>	$6.72 \pm 2.02^j$ (2.51) <sup>k</sup>	—	
	100–200	$0.09 \pm 0.02^j$ (0.05) <sup>k</sup>	$0.06 \pm 0.02^j$ (0.05) <sup>k</sup>	$0.63 \pm 0.33^j$ (0.09) <sup>k</sup>	—	

<sup>a</sup> Uncertainty not specified. <sup>b</sup> % diesel in vehicle fleet. <sup>c</sup> Median  $\pm$  Q (semi-quartile). <sup>d</sup> Mean  $\pm$  standard error. <sup>e</sup> 95% confidence interval. <sup>f</sup> Median  $\pm$  standard error. <sup>g</sup> Mean (IQR). <sup>h</sup> Median  $\pm$  median absolute deviation. <sup>i</sup> Daily mean (05:00–23:00). <sup>j</sup> Mean  $\pm$  standard deviation. <sup>k</sup> Most realistic value (sector D). <sup>l</sup> Typical motorway traffic conditions. <sup>m</sup> Typical urban traffic conditions with most vehicles traveling in a stop-start mode between two traffic lights.



the study by Birmili *et al.*<sup>9</sup> who estimated  $EF_{mf}$  by an inverse modelling approach close to the motorway A100 in Berlin (mean traffic driving speed of  $80 \text{ km h}^{-1}$ ), the present  $EF_{mf}$  for TNC is larger by about  $0.7 \times 10^{14} \text{ veh}^{-1} \text{ km}^{-1}$ . This is somewhat surprising as a lower emission factor may have been expected with respect to the assumption that a mixed urban vehicle fleet modernises in certain time intervals and that a higher share of vehicles with cleaner emission technology should be present nowadays in comparison to the Birmili *et al.*<sup>9</sup> study conducted about 14 years ago. However, it is difficult to compare both estimates as the one was conducted close to a motorway, over a short summer period of 10 weeks, and was measured over a larger diameter size range (*i.e.*  $10 < D_p < 500 \text{ nm}$ ), whereas the present study observed more typical urban driving patterns which may have been influenced by a higher share of congested traffic situations, especially during rush-hour traffic.

As stated in the introduction, our study aims to quantify a 'typical' mixed-fleet road traffic emission factor which is representative for urban Berlin. Hence, we focussed on the quantification of an average weekday situation with commuting traffic and excluded periods with 'non-typical' traffic situations such as weekends or holidays. Stratification of the data-set into specific situation such as seasonal variation (winter *vs.* summer particle EFs), or weekend *vs.* weekday comparison will result in smaller groups of data being subject to the regression approach (*cf.* eqn (5)). This would likely increase the variance in the data resulting in more uncertain particle EFs. The analysis of the potential of the regression method for estimation of more specific particle EFs, however, would be an interesting subject for future research. The derived emission factors for light and heavy duty vehicles are within the literature range of  $0.24\text{--}9.25 \times 10^{14} \text{ veh}^{-1} \text{ km}^{-1}$  for  $EF_{LDV}$  and  $6.6\text{--}42.0 \times 10^{14} \text{ veh}^{-1} \text{ km}^{-1}$  for  $EF_{HDV}$  (*cf.* Table 2). However, most other studies with a similar lower cut-off (*i.e.*  $D_p$  of 8–11 nm) report  $EF_{LDV}$  that are smaller by a factor of 5–7 compared to this study. The results of  $EF_{LDV}$  for Londrina, Brazil with  $9.25 (\pm 1.13) \times 10^{14} \text{ veh}^{-1} \text{ km}^{-1}$  (ref. 18) and for Minnesota, USA with  $6.2 (\pm 1.4) \times 10^{14} \text{ veh}^{-1} \text{ km}^{-1}$  are higher than at the Berlin site.<sup>39</sup> Our calculated  $EF_{HDV}$ , however, is in the range of estimates as reported by others and very close to figures reported for Stockholm, Sweden<sup>15</sup> and Copenhagen, Denmark.<sup>37</sup>

The finding that size-resolved particle emission factors for road traffic tend to increase with smaller particle diameters, is in agreement with our observations at the Berlin site as the largest particle emission factors were evident for the NUC mode, followed by the AIT mode (*e.g.*<sup>34,40</sup>).

## 4.2 Limitations of the study

When determining particle emission factors using linear and multiple linear regression of traffic activity and eddy covariance particle flux data (*cf.*<sup>15</sup>), the quality of the results depends on relationship between both quantities in the flux source area, *i.e.* the slope of the regression equation. Hence, the certainty of the emission factor should improve with the quality of the traffic data and the particle fluxes. In the present study, traffic activity was estimated using wind direction sectors covering an area of 2 km radius. Due to this rather simplified approach, an under-

overestimation of traffic activity cannot be ruled out, as roads in the sector have different traffic intensity, *i.e.* major and minor roads, and the flux source area is not homogeneously distributed across the 2 km study area.<sup>20</sup> This may result in a 'mismatch' between the variation in particle fluxes as driven from the flux source area *vs.* traffic intensity as estimated from the 2 km sector. Consequently, this will influence the certainty in the particle EF quantification.

An underestimation of traffic activity in a sector would lead to an increased slope of the regression line and thus to an increased emission factor. An overestimation, on the other hand, would lead to a lower emission factor. Due to the nearby "Straße des 17. Juni" to the north of the measurement station, which more significantly contributes to the particle flux than more distant areas within the 2 km radius, there may have been an underestimation of traffic activity in some sectors resulting in a slight overestimation of  $EF_{mf}$ . In sector D, which shows the highest amount of streets in the land-use of the flux source area (53%, *cf.*<sup>20</sup>) and is associated with the highest traffic activity of the six selected sectors, the estimated traffic activity therefore might be more certain than in the other sectors. More sophisticated flux source area modelling applying a source area-weighted estimation of traffic intensity may decrease uncertainty in the traffic estimation and consequently in the particle EF.<sup>41</sup>

Flux source area-weighted modelling may also help improving annual trend estimation of particle EFs as in the current state the annual differences are lower than the variation across the sectors A–F, *i.e.* the coefficient of variation (*cf.* Section 3.3). This implies that robust temporal trends cannot be derived from the present data. Temporal variation of particle fluxes, however, such as differences between the different observation years, might be associated with spatial shifts of the peak contribution location of the flux source area during the observation years. In a previous study we documented that in the second year, for instance, the average wind direction and also the peak flux source area shifted towards areas with lower traffic intensity, *i.e.* north-westerly directions.<sup>20</sup>

The transition of the mixed traffic fleet towards a higher fraction of low-emission standards or electric vehicles poses further variation of particle fluxes, as the proportion of electric vehicles in Berlin increased by a factor of 3 in the time period from 2017 to 2020.<sup>20</sup> However, the estimation of this influence would require more specific data such as the share of electric vehicles at hourly resolution, which were not available for the present analysis.

## 5 Summary and conclusions

Size-resolved particle emission factors were derived from 3 years of eddy-covariance particle number flux observations in Berlin, Germany. The averaged emission factor of  $EF_{mf} = 2.83 \times 10^{14} \text{ veh}^{-1} \text{ km}^{-1}$  for TNC is in the range of road traffic emission factors as reported in literature. The results indicate strongest particle emission from the mixed fleet to occur in the nucleation mode, *i.e.* 69% of total mixed fleet particle emission. The analysis for LDV and HDV indicated significantly higher  $EF_{HDV}$  than  $EF_{LDV}$  with, for instance, ratios of  $EF_{HDV}/EF_{LDV} = 11.2$  for UFP, and 9.8 for NUC. However, some



uncertainty in the calculation of emission factors arises from the estimation of sector-wise traffic activity, as this influences the slope of the regression equations to quantify particle emission factors. The study demonstrates the method of linear (multiple) regression between eddy covariance fluxes and traffic data to be a promising tool to derive particle emission factors for a vehicle fleet in the source area of eddy-covariance flux measurements. The method relies on the quality of both, the particle flux data and the traffic activity in the flux source area. The latter was estimated by a simplified approach in the present study which leaves some room for future improvement.

Generally, eddy covariance particle flux measurements prove a powerful tool to quantify (size-resolved) particle emission factors. Long-term measurements may help to study annual variation and trends in emission factors and may help to monitor the effects of the modernisation of the traffic fleet or traffic reduction measures on urban air quality.

## 6 Appendix



Fig. 8 Panoramic views of the site surroundings taken from rooftop of Technische Universität Berlin. (Top) The picture shows the areas northeast and west ( $270^{\circ}$ – $80^{\circ}$ ) of the site, (bottom) the area east and south ( $90^{\circ}$ – $260^{\circ}$ , pictures: Stephan Weber).

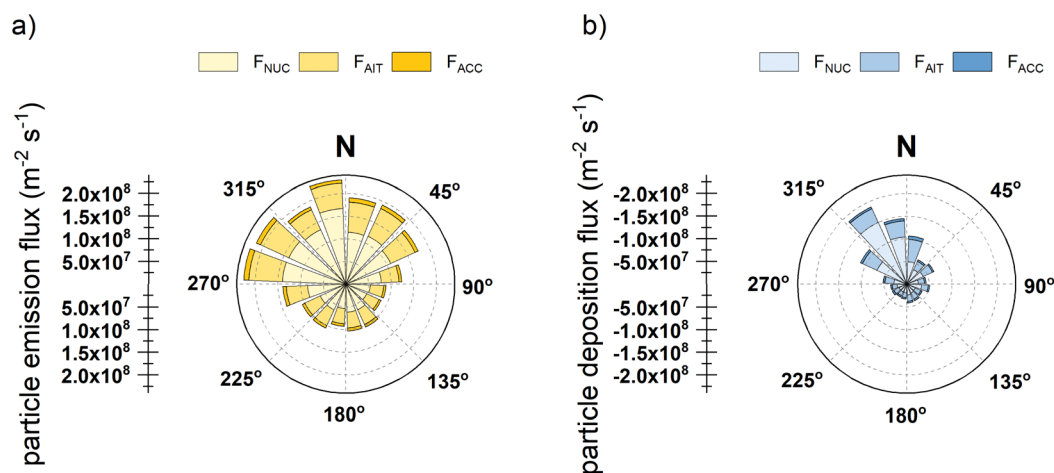


Fig. 9 Average (a) emission and (b) deposition particle number fluxes in the different wind sectors for nucleation ( $F_{\text{NUC}}$ ), Aitken ( $F_{\text{AIT}}$ ), and accumulation ( $F_{\text{ACC}}$ ) mode fluxes (Straaten and Weber, 2021).<sup>20</sup>



## Conflicts of interest

There are no conflicts to declare.

## Acknowledgements

We would like to thank Daniel Weber from Senate Department for the Environment, Urban Mobility, Consumer Protection and Climate Action of the Berlin city administration for providing hourly traffic data from 22 traffic counting stations in the study area. We further thank our project partners (Dieter Scherer and Fred Meier) of the Chair of Climatology, Institute of Ecology, Technische Universität Berlin for the opportunity to conduct long-term particle flux measurements at their urban climate observatory. Another thank goes to Hagen Mittendorf of Technische Universität Braunschweig for supporting the flux site maintenance. This study was supported by the German Federal Ministry of Education and Research (BMBF; grant nos. FKZ 01 LP 1602 D – Urban Climate Under Change, Module 3DO – and FKZ 01 LP 1912 D – Urban Climate Under Change, phase II, Module 3DO+M).

## References

- 1 P. Kumar, L. Morawska, W. Birmili, P. Paasonen, M. Hu, M. Kulmala, R. M. Harrison, L. Norford and R. Britter, Ultrafine particles in cities, *Environ. Int.*, 2014, **66**, 1–10.
- 2 C. von Bismarck-Osten, W. Birmili, M. Ketzler, A. Massling, T. Petäjä and S. Weber, Characterization of parameters influencing the spatio-temporal variability of urban aerosol particle number size distributions in four European cities, *Atmos. Environ.*, 2013, **77**, 415–429.
- 3 M. C. Simon, N. Hudda, E. N. Naumova, J. I. Levy, D. Brugge and J. L. Durant, Comparisons of traffic-related ultrafine particle number concentrations measured in two urban areas by central, residential, and mobile monitoring, *Atmos. Environ.*, 2017, **169**, 113–127.
- 4 I. Rivas, D. C. S. Beddows, F. Amato, D. C. Green, L. Järvi, C. Hueglin, C. Reche, H. Timonen, G. W. Fuller, J. V. Niemi, N. Pérez, M. Aurela, P. K. Hopke, A. Alastuey, M. Kulmala, R. M. Harrison, X. Querol and F. J. Kelly, Source apportionment of particle number size distribution in urban background and traffic stations in four European cities, *Environ. Int.*, 2020, **135**, 105345.
- 5 S. Ohlwein, R. Kappeler, M. Kutlar Joss, N. Künzli and B. Hoffmann, Health effects of ultrafine particles: a systematic literature review update of epidemiological evidence, *Int. J. Public Health*, 2019, **64**(4), 547–559.
- 6 H.-S. Kwon, M. H. Ryu and C. Carlsten, Ultrafine particles: unique physicochemical properties relevant to health and disease, *Exp. Mol. Med.*, 2020, **52**(3), 318–328, DOI: [10.1038/s12276-020-0405-1](https://doi.org/10.1038/s12276-020-0405-1).
- 7 European Commission, *Proposal for a Directive of the European Parliament and of the Council on Ambient Air Quality and Cleaner Air for Europe*, 2022, 542 final/2, p. 75.
- 8 L. Morawska, Z. Ristovski, E. R. Jayaratne, D. U. Keogh and X. Ling, Ambient nano and ultrafine particles from motor vehicle emissions: Characteristics, ambient processing and implications on human exposure, *Atmos. Environ.*, 2008, **42**(35), 8113–8138.
- 9 W. Birmili, B. Alaviippola, D. Hinneburg, O. Knoth, T. Tuch, J. Borken-Kleefeld and A. Schacht, Dispersion of traffic-related exhaust particles near the Berlin urban motorway – estimation of fleet emission factors, *Atmos. Chem. Phys.*, 2009, **9**(7), 2355–2374, DOI: [10.5194/acp-9-2355-2009](https://doi.org/10.5194/acp-9-2355-2009).
- 10 P. Brimblecombe, T. Townsend, C. F. Lau, A. Rakowska, T. L. Chan, G. Močnik and Z. Ning, Through-tunnel estimates of vehicle fleet emission factors, *Atmos. Environ.*, 2015, **123**, 180–189.
- 11 Y. Fujitani, K. Takahashi, A. Fushimi, S. Hasegawa, Y. Kondo, K. Tanabe and S. Kobayashi, Particle number emission factors from diesel trucks at a traffic intersection: Long-term trend and relation to particle mass-based emission regulation, *Atmos. Environ.: X*, 2020, **5**, 100055.
- 12 L. Gerling and S. Weber, Mobile measurements of atmospheric pollutant concentrations in the pollutant plume of BER airport, *Atmos. Environ.*, 2023, **304**, 119770.
- 13 L. Morawska, M. Jamriska, S. Thomas, L. Ferreira, K. Mengersen, D. Wraith and F. McGregor, Quantification of particle number emission factors for motor vehicles from on-road measurements, *Environ. Sci. Technol.*, 2005, **39**(23), 9130–9139, DOI: [10.1021/es050069c](https://doi.org/10.1021/es050069c).
- 14 A. M. Jones and R. M. Harrison, Estimation of the emission factors of particle number and mass fractions from traffic at a site where mean vehicle speeds vary over short distances, *Atmos. Environ.*, 2006, **40**(37), 7125–7137.
- 15 E. M. Mårtensson, E. D. Nilsson, G. Buzorius and C. Johansson, Eddy covariance measurements and parameterisation of traffic related particle emissions in an urban environment, *Atmos. Chem. Phys.*, 2006, **6**, 769–785, DOI: [10.5194/acp-6-769-2006](https://doi.org/10.5194/acp-6-769-2006).
- 16 S. Janhäll, P. Molnar and M. Hallquist, Traffic emission factors of ultrafine particles: effects from ambient air, *J. Environ. Monit.*, 2012, **14**(9), 2488–2496.
- 17 V. Franco, M. Kousoulidou, M. Muntean, L. Ntziachristos, S. Hausberger and P. Dilara, Road vehicle emission factors development: A review, *Atmos. Environ.*, 2013, **70**, 84–97.
- 18 P. Krecl, A. C. Targino, T. P. Landi and M. Ketzler, Determination of black carbon, PM<sub>2.5</sub>, particle number and NO<sub>x</sub> emission factors from roadside measurements and their implications for emission inventory development, *Atmos. Environ.*, 2018, **186**, 229–240, DOI: [10.1016/j.atmosenv.2018.05.042](https://doi.org/10.1016/j.atmosenv.2018.05.042).
- 19 L. Järvi, C. S. B. Grimmond and A. Christen, The Surface Urban Energy and Water Balance Scheme (SUEWS): Evaluation in Los Angeles and Vancouver, *J. Hydrol.*, 2011, **411**(3–4), 219–237, DOI: [10.1016/j.jhydrol.2011.10.001](https://doi.org/10.1016/j.jhydrol.2011.10.001).
- 20 A. Straaten and S. Weber, Measurement report. Three years of size-resolved eddy-covariance particle number flux measurements in an urban environment, *Atmos. Chem. Phys.*, 2021, **21**(24), 18707–18726, DOI: [10.5194/acp-2021-625](https://doi.org/10.5194/acp-2021-625).
- 21 D. Scherer, F. Ament, S. Emeis, U. Fehrenbach, B. Leidl, K. Scherber, C. Schneider and U. Vogt, Three-Dimensional



- Observation of Atmospheric Processes in Cities, *Metz*, 2019, **28**, 121–138, DOI: [10.1127/metz/2019/0911](https://doi.org/10.1127/metz/2019/0911).
- 22 J. A. Quanz, Impact of spatial heterogeneity on energy exchange in an urban environment in Berlin, Germany, Master thesis, Technische Universität Berlin, 2018, p. 85.
- 23 Geoportal Berlin, Biotope types, license “dl-de/by-2-0”, 2014. Available at: <https://www.berlin.de/umweltatlas/en/biotopes/biotope-types/continually-updated/summary/>, accessed July 2023; Traffic volumes 2019, license “dl-de/by-2-0”, available at: <https://www.berlin.de/umweltatlas/en/traffic-noise/traffic-volumes/2019/summary/>, accessed July 2023; ALKIS Berlin Building types, license “dl-de/by-2-0”, available at: <https://daten.berlin.de/datensaetze/alkis-berlin-geb%C3%A4ude-wfs>, accessed July 2023.
- 24 A. Meyer-Kornblum, L. Gerling and S. Weber, Gap-filling fast electrical mobility spectrometer measurements of particle number size distributions for eddy covariance application, *Aerosol Air Qual. Res.*, 2019, **19**(12), 2721–2731, DOI: [10.4209/aaqr.2019.06.0291](https://doi.org/10.4209/aaqr.2019.06.0291).
- 25 W. C. Hinds, *Aerosol Technology, Properties, Behavior, and Measurement of Airborne Particles*, Wiley, New York, 2nd edn, 1999.
- 26 D. Vickers and L. Mahrt, Quality control and flux sampling problems for tower and aircraft data, *J. Atmos. Ocean. Technol.*, 1997, **14**(3), 512–526, DOI: [10.1175/1520-0426\(1997\)014<0512:QCAFSP>2.0.CO;2](https://doi.org/10.1175/1520-0426(1997)014<0512:QCAFSP>2.0.CO;2).
- 27 J. B. Moncrieff, J. M. Massheder, H. de Bruin, J. Elbers, T. Friberg, B. Heusinkveld, P. Kabat, S. Scott, H. Soegaard and A. Verhoef, A system to measure surface fluxes of momentum, sensible heat, water vapour and carbon dioxide, *J. Hydrol.*, 1997, **188–189**, 589–611.
- 28 J. Moncrieff, R. Clement, J. Finnigan and T. Meyers, Averaging, detrending, and filtering of eddy covariance time series, in *Handbook of Micrometeorology*, ed. Lee X., Massman W. and Law B., Springer, Dordrecht, Atmos. Ocean. Sci. Lib. 29, 2004.
- 29 T. W. Horst, A simple formula for attenuation of eddy fluxes measured with first-order response scalar sensors, *Bound.-Layer Meteorol.*, 1997, **82**(2), 219–233, DOI: [10.1023/A:1000229130034](https://doi.org/10.1023/A:1000229130034).
- 30 T. Foken, M. Göockede, M. Mauder, L. Mahrt, B. Amiro and W. Munger, in *Post-Field Data Quality Control (Handbook of Micrometeorology)*, ed. Lee X., Massman W. and Law B., Springer, Dordrecht, Atmos. Ocean. Sci. Lib. 29, 2004.
- 31 L. Gerling and S. Weber, Atmospheric transformation of urban particle number size distributions during the transport along street canyons as quantified by an aerosol sectional model, *Atmos. Pollut. Res.*, 2022, **13**(2), 101296.
- 32 C. F. Dormann, J. Elith, S. Bacher, C. Buchmann, G. Carl, G. Carré, J. Marquéz, B. Gruber, B. Lafourcade, P. J. Leitão, T. Münkemüller, C. McClean, P. E. Osborne, B. Reineking, B. Schröder, A. K. Skidmore, D. Zurell and S. Lautenbach, Collinearity: a review of methods to deal with it and a simulation study evaluating their performance, *Ecography*, 2013, **36**(1), 27–46.
- 33 M. J. Deventer, L. von der Heyden, C. Lamprecht, M. Graus, T. Karl and A. Held, Aerosol particles during the Innsbruck Air Quality Study (INNAQS): Fluxes of nucleation to accumulation mode particles in relation to selective urban tracers, *Atmos. Environ.*, 2018, **190**, 376–388, DOI: [10.1016/j.atmosenv.2018.04.043](https://doi.org/10.1016/j.atmosenv.2018.04.043).
- 34 M. Conte and D. Contini, Size-resolved particle emission factors of vehicular traffic derived from urban eddy covariance, *Environ. Pollut.*, 2019, **251**, 830–838, DOI: [10.1016/j.envpol.2019.05.029](https://doi.org/10.1016/j.envpol.2019.05.029).
- 35 D. W. Kittelson, W. F. Watts and J. P. Johnson, Nanoparticle emissions on Minnesota highways, *Atmos. Environ.*, 2004, **38**, 9–19, DOI: [10.1016/j.atmosenv.2003.09.037](https://doi.org/10.1016/j.atmosenv.2003.09.037).
- 36 M. Ketzler, P. Wählin, R. Berkowicz and F. Palmgren, Particle and trace gas emission factors under urban driving conditions in Copenhagen based on street and roof-level observations, *Atmos. Environ.*, 2003, **37**, 2735–2749, DOI: [10.1016/S1352-2310\(03\)00245-0](https://doi.org/10.1016/S1352-2310(03)00245-0).
- 37 F. Wang, M. Ketzler, T. Ellermann, P. Wahlin, S. S. Jensen, D. Fang and A. Massling, Particle number, particle mass and NOx emission factors at a highway and an urban street in Copenhagen, *Atmos. Chem. Phys.*, 2010, **10**, 2745–2764, DOI: [10.5194/acp-10-2745-2010](https://doi.org/10.5194/acp-10-2745-2010).
- 38 D. Contini, A. Donato, C. Elefante and F. M. Grasso, Analysis of particles and carbon dioxide concentrations and fluxes in an urban area, *Atmos. Environ.*, 2019, **46**, 25–35, DOI: [10.1016/j.atmosenv.2022.10.039](https://doi.org/10.1016/j.atmosenv.2022.10.039).
- 39 J. P. Johnson, D. B. Kittelson and W. F. Watts, Source apportionment of diesel and spark ignition exhaust aerosol using on-road data from the Minneapolis metropolitan area, *Atmos. Environ.*, 2005, **39**, 2111–2121, DOI: [10.1016/j.atmosenv.2004.12.018](https://doi.org/10.1016/j.atmosenv.2004.12.018).
- 40 C. Nickel, H. Kaminski, B. Hellack, U. Quass, A. John, O. Klemm and T. A. J. Kuhlbusch, Size resolved particle number emission factors of motorway traffic differentiated between heavy and light duty vehicles, *Aerosol Air Qual. Res.*, 2013, **13**(2), 450–461, DOI: [10.4209/aaqr.2012.07.0187](https://doi.org/10.4209/aaqr.2012.07.0187).
- 41 H. Chu, X. Luo, Z. Ouyang, W. S. Chan, S. Dengel, S. C. Biraud, M. S. Torn, S. Metzger, J. Kumar, M. A. Arain, T. J. Arkebauer, D. Baldocchi, C. Bernacchi, D. Billesbach, T. A. Black, P. D. Blanken, G. Bohrer, R. Bracho, S. Brown, N. A. Brunzell, J. Chen, X. Chen, K. Clark, A. R. Desai, T. Duman, D. Durden, S. Fares, I. Forbrich, J. A. Gamon, C. M. Gough, T. Griffis, M. Helbig, D. Hollinger, E. Humphreys, H. Ikawa, H. Iwata, Y. Ju, J. F. Knowles, S. H. Knox, H. Kobayashi, T. Kolb, B. Law, X. Lee, M. Litvak, H. Liu, J. W. Munger, A. Noormets, K. Novick, S. F. Oberbauer, W. Oechel, P. Oikawa, S. A. Papuga, E. Pendall, P. Prajapati, J. Prueger, W. L. Quinton, A. D. Richardson, E. S. Russell, R. L. Scott, G. Starr, R. Staebler, P. C. Stoy, E. Stuart-Haëntjens, O. Sonnentag, R. C. Sullivan, A. Suyker, M. Ueyama, R. Vargas, J. D. Wood and D. Zona, Representativeness of Eddy-Covariance flux footprints for areas surrounding AmeriFlux sites, *Agric. For. Meteorol.*, 2021, **301–302**, 108350.



- 42 L. Järvi, Ü. Rannik, I. Mammarella, A. Sogachev, P. P. Aalto, P. Keronen, E. Siivola, M. Kulmala and T. Vesala, Annual particle flux observations over a heterogeneous urban area, *Atmos. Chem. Phys.*, 2009, **9**(3), 13407–13437, DOI: [10.5194/acpd-9-13407-2009](https://doi.org/10.5194/acpd-9-13407-2009).
- 43 J. L. Perkins, L. T. Padró-Martínez and J. L. Durant, Particle number emission factors for an urban highway tunnel, *Atmos. Environ.*, 2013, **74**, 326–337, DOI: [10.1016/j.atmosenv.2013.03.046](https://doi.org/10.1016/j.atmosenv.2013.03.046).
- 44 N. Raparathi, S. Debbarma and H. C. Phuleria, Development of real-world emission factors for on-road vehicles from motorway tunnel measurements, *Atmos. Environ.: X*, 2021, **10**, 100113, DOI: [10.1016/j.aeaoa.2021.100113](https://doi.org/10.1016/j.aeaoa.2021.100113).

